CHAPTER 5: THE INITIAL FORMATION OF MOUND SPRING STRUCTURES: INSIGHTS FROM CARBONATE REACTIVE TRANSPORT MODELLING

This chapter is based on the following presentation and peer reviewed report:

Keppel, M. Halihan, T., Love, A., Post, V., Werner, A. D., Clarke, J., 2013 a. Chapter 3: Formation and evolution of mound springs. In: Love, A.J., Shand, P., Crossey, L.J., Harrington, G.A., Rousseau-Gueutin, P. (Eds.), Groundwater Discharge of the Western Margin of the Great Artesian Basin, Australia. 3, National Water Commission, Canberra.

Keppel, M.N., Post, V., Werner, A. D., Love, A., Clarke, J., Halihan, T., 2012a. The use of water balance and carbonate reaction modelling to predict the initial formation of mound spring structures, central South Australia, International Association of Hydrogeologists 2012 Congress. International Association of Hydrogeologists, Niagara Falls, Canada.

Abstract

Mound springs are dome-shaped structures composed predominantly of $CaCO_3$ associated with discharging groundwater from the GAB. To explain how these structures initially form, a reactive transport hydrochemistry and water balance model was applied. A variety of discharge rates and different mound sizes were modelled using measured major ion chemistry. It was found that the mound footprint predicted by the model generally provided a reasonable approximation of the measured mound footprint. Differences between predicted and measured mound

footprints may be indicative of gross changes in discharge rate from a given spring over time. The work presented here provides a "proof of concept" in that the provision of predictions concerning the spatial footprint through carbonate-reaction modelling that reasonably replicate the measured footprint of a spring-related structure can be used to impart quantitative constraints on determinations of past spring activity. Additionally, the footprint of calcareous mound spring structures is conceptualised as being primarily a product of carbonate precipitation, although the sensitivity of the model to discharge suggests this is also influential. Consequently, the application of carbonate-reaction hydrochemistry modelling as a means of explaining initial mound formation, combined with age-dating of material from calcareous spring deposits, may have application as a palaeohydrological tool.

.

5.1 Introduction

Mound springs are dome-shaped structures built from calcareous spring deposits. They are found around the world (Linares et al., 2010; Pentecost, 1995) and can be culturally and ecologically invaluable environments that necessitate safeguarding against the impacts of groundwater exploitation (Ah Chee, 2002; Leek, 2002; Mudd, 2000) and surface excavation. More recently, similar-looking structures have been identified on Mars (Allen and Oehler, 2008; Bourke et al., 2007; Clarke and Bourke, 2010); their manifest similarity has led to comparable hypotheses concerning formation via groundwater discharge (Allen and Oehler, 2008; Bourke et al., 2007). Palaeoclimatic reconstructions using similar calcareous terrestrial spring deposits (Andrews et al., 2000; Anzalone et al., 2007; Hori et al., 2009), require an understanding of the processes that control mound spring formation. Although conceptual models for formation have been previously proposed (Chapter 3; Kerr and Turner, 1996; Pentecost and Viles, 1994; Williams and Holmes 1978), little work has been attempted with respect to quantifying controls on accumulation since Williams and Holmes (1978) used a mass balance approach to roughly estimate a mound accumulation timescale. A notable exception was Nelson et al. (2007) who used a hydraulics-based model to describe the physical accumulation and subsequent morphology of mound springs for field sites at Dalhousie Springs, located approximately 300 km to the north of the Lake Eyre South region. However, a stated caveat in Nelson et al. (2007) was that a physical model was being used to describe a process that occurs chemically and consequently a number of important assumptions concerning the chemistry of carbonate precipitation were being made, including temperature dependence of carbonate precipitation. Likewise, there have been other attempts at describing the controls on the spatial extent of carbonate precipitation

within terrestrial spring environments (e.g. Chan and Goldenfeld, 2007; Goldenfeld et al., 2006; Hammer et al., 2007; Jettestuen et al., 2006) such studies primarily focus on either thermogene environments in a similar way to Nelson et al. (2007) or accumulation and micro-scales and are therefore not readily applicable to assessing meso-scale, near-ambient meteogene, calcareous spring environments such as the Lake Eyre South mound springs. This work tests if reactive transport modelling can provide a quantitative framework to place constraints on terrestrial carbonate depositing environments such as mound springs. This is demonstrated by modifying a quantitative model of the depositional environment of mound springs (Chapter 4) to simulate their early formation. Consequently, the spatial extent of mound structures can be predicted based on the concentrations of precipitating solutes and the magnitude of spring discharge.

Dating techniques in combination with stable oxygen and carbon isotope analysis of fossiliferous calcareous spring deposits have been used to derive changes in climate and the onset of arid periods within the recharge areas that supply springs (Andrews et al., 2000; Anzalone et al., 2007; Brookes, 1993; Crombie et al., 1997; Evans, 1999; Hori et al., 2009; Miner et al., 2007). Furthermore, the impact of past climate change on carbonate precipitation through a synthesis of various hydrologic, water chemistry and geophysical data has also been studied (Dilsiz et al., 2004; Valero Garces et al., 2008). Calcareous spring deposits may hold further information about the long-term temporal dynamics of spring discharge. Knowledge of long-term variations of spring discharge has particular pertinence to the protection and management of springs especially in arid and semi-arid areas. For example, the mound springs of the Lake Eyre South region in Australia, which are studied here,

sustain unique wetland ecosystems and are of invaluable cultural significance (Ah Chee, 2002; Leek, 2002). They are potentially threatened by groundwater exploitation by pastoral and mining industries (Mudd, 2000; Thomson and Barnett, 1985), but without knowledge of the natural variations of spring discharge, it is difficult to assess the impact of these activities.

Consequently, a clear need to use calcareous spring deposits as archives of past environmental conditions exists; however, it is essential to have a clear understanding of the fundamental geochemical and sedimentological processes that control deposition (Andrews et al., 2000; Jones, 2010). While field-based studies abound in the literature, reactive transport modelling has so far not been used to quantify past mound spring environments. An investigation into whether reactive transport modelling can be used to place quantitative constraints on the spatial extent of spring discharge and carbonate precipitation, using the mound springs in the Lake Eyre South region as a study area is presented herein. Such modelling provides a process-based quantitative description of the geochemical processes controlling the footprint of mound springs. By focussing on the first stage of mound formation, the model could be used to estimate the initial discharge conditions responsible for the formation of ancient mound structures (Prescott and Habermehl, 2008) comparison of such modelled conditions to those encountered today may provide useful palaeohydrological information concerning the spring and aquifer system in question.

5.2 Study Area

Five calcareous mound springs from the Lake Eyre South region of South Australia were investigated during this study (Figure 5.1). Study sites were limited to those

with identifiable singular vent and mound structures, adequate aerial photographic coverage and reliable recent discharge and hydrochemistry data.

The investigated springs are generally dome-shaped (Figure. 5.2a), however, two larger springs (Warburton and The Bubbler) have larger, shield-like structures (Figure 5.2b); most are part of a wider calcareous apron (Figure 5.2a). Their height varies from 2 to 5 m from base to peak and have central pools that vary from being sparsely to well vegetated. Where exposed, carbonate bedding appears laminar, composed of plant or microbial tufa (Chapter 3) up to several centimetres thick.

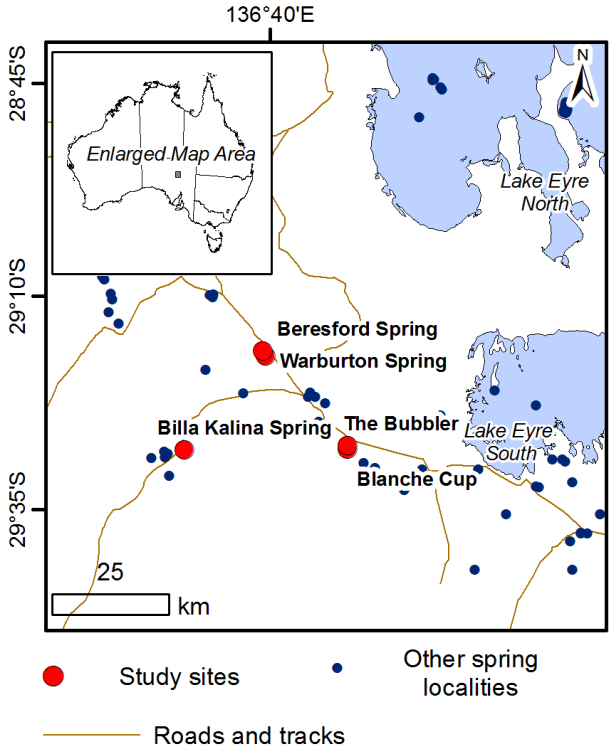

Figure 5.1: Location map of study sites. Inset show location in Australia.

The near circular shape of the mound deposits indicates that they initially formed by carbonate precipitation from discharging groundwater with radial discharge away from the spring vent. Modelling assumptions therefore include radial symmetry as well as steady state discharge conditions based on a balance between spring discharge and water loss by evapotranspiration and estimated infiltration. Discharge for each spring, the spatial extent and water loss characteristics used in modelling are provided in Table 5.1.

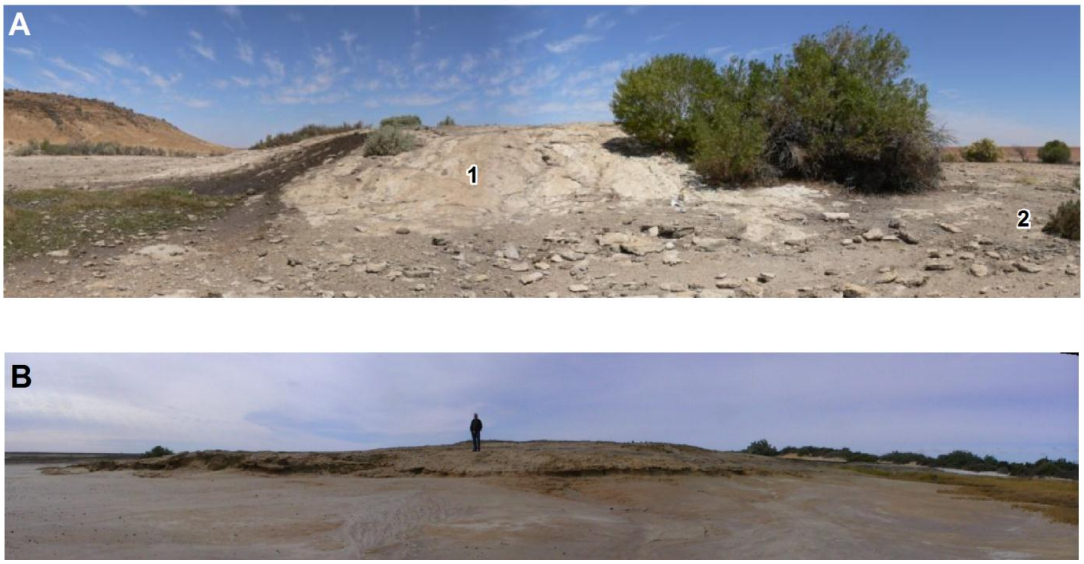

Figure 5.2: Photographs describing morphology of mound spring structures. a) Photograph of the mound spring at Beresford springs. Beresford is typical of a low-discharge (<1 L/sec) spring. The mound structure (1) is the steeply-walled, tufa dome, as opposed to the calcareous apron surrounding the mound (2). b) Photograph of the tufa mound at The Bubbler. The Bubbler is typical of a high-discharge (>1 L/sec) spring and the resultant mound has a shield-like form.

Table 5.1: Characteristics of mound spring study sites. Spatial data obtained via aerial photograph interpretation and measurements collected during field works conducted between October 2009 and July 2010. Evapotranspiration and infiltration were estimated using the average of those published for warmer and cooler periods presented in Chapter 4 and Keppel et al. (2012b).

Spring	Abr.	Disch. *(Q)* L/sec	Surface area of modern wetland m^2	Surface area mound base m^2	Total water-loss mm/ day	Estimated loss: *E.T.* mm/day	Estimated loss: Infiltration mm/day
Beresford	B	0.06	840	2,308	6.2	2.0	4.1
Warburton	W	3.08	16,000	6,713	16.2	5.3	10.9
The Bubbler	TB	9.25	38,500	4,960	22.4	7.4	15.0
Blanche Cup	BC	0.25	1,400	3,023	15.4	5.2	10.3
Billa Kalina	BK	0.21	930	471	19.5	9.2	13.1

5.3 Methodology

5.3.1 Field methods

Field techniques used to obtain water samples were described in Chapter 4. The spatial extent of the mound springs and the features of the surrounding terrain were mapped using stereoscopic pairs of aerial photographs obtained from DEH. The exceptions to this was Billa Kalina Springs, where only single images were available; however, the prominence of the mounds compared to the surrounding landscape at this site made mapping viable. From this, the area of the mound footprint was calculated using the Geographical information Systems (GIS) software package "ArcMap^{TM}". Using this area, the effective radius of each mapped mound was calculated as if the surface area was circular; this estimated average mound radius was then compared to those predicted using carbonate-reaction modelling. All interpretations were verified in the field using GPS.

5.3.2 Carbonate-reaction modelling - Theoretical considerations

The hydrochemical transport model from Chapter 4 was modified to test if it could predict the surface area of the base of a mound during the initial stage of mound development, based on the measured chemical composition and discharge rate of the springwater. The model calculates the changing chemical composition of the water as it flows away from the spring vent under the influence of (i) CO_2 degassing by either physio-chemical mechanisms or biomediation (ii) $CaCO_3$ precipitation or dissolution and (iii) evapotranspiration.

Based on evidence presented in Chapter 3, it was assumed that from initial formation, the resultant spring wetland will be colonised by dense sedge and reed vegetation quickly compared to the time estimated to construct an average mound, which may take at least hundreds of years (Williams and Holmes, 1978). The near circular shape of the mounds suggests that they initially formed by carbonate precipitation from discharging groundwater that flowed away from the spring vent in a radial fashion. Consequently, the geometry of the earliest stage surface manifestation of a mound spring was conceptualised as a circular pool (Figure 5.3), i.e., discharging water flows away in a radial fashion from the vent. This assumption was justified given the flat topography of the terrain, and the observed circular shape of existing mound springs. As in the case for modern mound spring wetland environments described in Chapter 4, steady state discharge conditions were assumed, i.e., the volumetric discharge rate of the spring Q (L^3/T) equals the total volumetric loss rate of water lost via evapotranspiration (ET, L^3/T) and infiltration (In, L^3/T) over the extent of the circular wetland ($Q = ET+In$). The evapotranspiration flux e (L/T) and infiltration flux i (L/T) was assumed to be spatially uniform and constant in time.

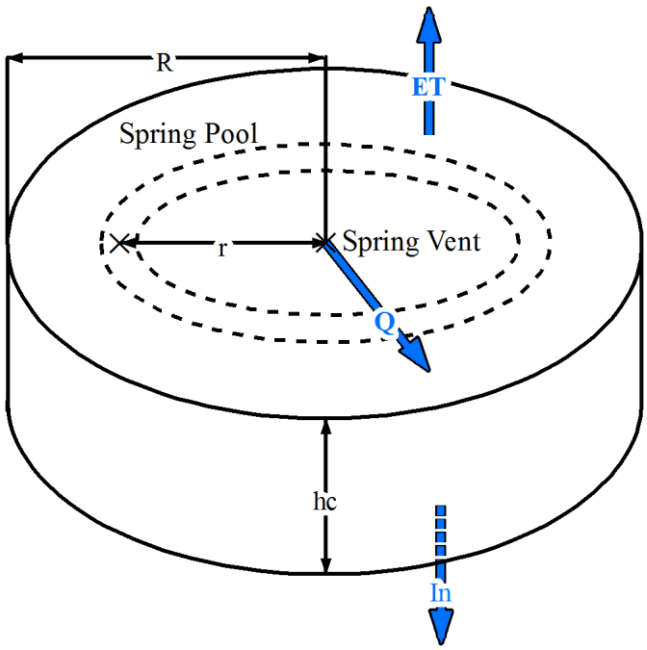

Figure 5.3: Graphical representation of the geometry-based hydrochemistry model used to simulate $CaCO_3$ precipitation within the initial mound spring environment. *R* is the maximum radius the spring pool can obtain, *r* is the distance to a designated cell area, *Q* is the initial water discharge, *ET* and *In* are water-loss through evaporation and infiltration respectively and h_c is the height of the water column.

In addition to the water balance, the flow mechanics of such a spring-fed wetland environment are important to understand before modelling is attempted. According to Kadlec et al. (1981), flow within a shallow wetland may be described as slow, gravitationally controlled flow through a doubly porous medium; porosity is composed of a small scale storage porosity related to water within plant stems, detritus and litter and a coarse scale blockage porosity formed by saturated plant and detrital hummocks, islets and channels. Although there have been numerous approaches with respect to modelling the friction effects of vegetation and detritus in wetlands (Tsihrintzis and Madieo, 2000) the law described by Kadlec (1981) and Kadlec (1990) appeared the most adaptable for shallow wetlands with laminar flow characteristics as observed at mound springs:

$$q = K_w h^b S^a = v h_c \quad (1)$$

Where q is discharge per unit width (L^2/T), K_w is the hydraulic conductance coefficient for overland flow ($L^2/T.L^b$), h is the height of the surface water column at a given point (L), v is the average superficial velocity of flow, h_c is the average depth of the "free" surface water column over the wetland (also defined as the surface water volume divided by the inundated area), r is the radial distance to a given point (L), S is the hydraulic gradient ($\partial h/\partial r$), b is an exponent related to vegetation microtopography, stem depth and density distribution and a is an exponent that describes the degree of either laminar or turbulent flow conditions (Chin, 2006).

Consequently, steady state radial flow through a shallow wetland similar to what may be anticipated during the initial stages of mound spring development could be described using a combination of this friction law with a mass balance equation, adapted from Hammer and Kadlec (1986):

$$\frac{\partial}{\partial r} 2\pi r (K_w h^b S^a) = Q - \pi(e + i) r^2 \quad (2)$$

In addition to evapotranspiration, the other important chemical reactions that occur as springwater flows away from the vent include degassing of dissolved CO_2 and calcite ($CaCO_3$) precipitation. $CaCO_3$ precipitation was modelled using the kinetic rate equation by Plummer et al. (1978), while the loss of CO_2 to atmosphere by degassing was described using the following rate expression (Bennett and Rathbun, 1972):

$$rc_T = k(CO_2 - CO_{2(eq)}) \quad (3)$$

Where rc_T is the reaction term for CO_2 (mol/sec) transfer from water to atmosphere, k is the gas exchange rate constant, CO_2 (mol) is the actual aqueous CO_2 concentration and $CO_{2(eq)}$ (mol) is the equilibrium aqueous CO_2 concentration. A k value of 4.5 x 10^{-4}/sec was used in all examples and represents an average of those previously published in Keppel et al. (2012b) and presented in Chapter 4. This value was also within the range of published values for stream environments (Choi et al., 1998; Genereux and Hemond, 1992; Longsworth, 1991).

5.3.3 Carbonate-reaction modelling- application

Using the assumptions regarding steady-state discharge and flow mechanics described above, the maximum radius of the wetland follows from:

$$R = \sqrt{\left(\frac{Q}{\pi(e+i)}\right)} \quad (4)$$

Where R is the maximum radius of the wetland (L).

Hydrochemical modelling was performed using PHREEQC-2, which uses a mixing-cell approach to simulate transport along a flow-line with a constant residence time in each cell (Parkhurst and Appelo, 1999). In the radial flow situation considered, the progressive decrease in water flow velocity as a function of water loss could be approximated using equation (2). This was done by assuming that the surface area of the initial wetland was completely inundated and using the average water column height h_c, which allows the friction law term to be replaced by $v.h_c$ according to equation (1). Rearranging the formula produces:

$$v(r) = \frac{Q-\pi(e+i)r^2}{2\pi h_c r} \quad (5)$$

The constant h_c was obtained by solving equation (2) for *h* with consideration to boundary conditions concerning the state of flow at the centre of radial discharge $[2\pi rhv]_{r=0} = Q$, and the condition of dryness beyond the maximum extent of the wetland $[Q=0, h=0]_R$. The resulting solution for steady state radial flow for a mound spring environment was determined as follows (Kadlec pers.comm., 2012):

$$h^{b+1} = \frac{b+1}{K_w}\left[\frac{Q}{2\pi} ln \frac{R}{r} - (e+i)\left(\frac{R^2-r_0^2}{4}\right)\right] \quad (6)$$

By using equation (6) to calculate *h* at 1 m intervals from the point of spring discharge to the edge of the wetland, the value of h_c was derived as the average of the resultant *h* values. Based on the previously stated assumptions concerning dense vegetation coverage and shallow, laminar flow conditions, values of 1 and 3 for the exponents *a* and *b* and a K_w value of 1.0 x 10^7 /m.day were adopted, with these figures obtained from field-based experiments conducted in wetland environments with similar characteristics (Kadlec et al, 1981; Kadlec and Wallace, 2009; Tsihrintzis and Madiedo, 2000).

As stated previously in Chapter 4, the flow velocity in PHREEQC-2 was defined implicitly based on a fixed transport time step length and the length of a grid cell. Cell lengths can be found by noting that $v(r) = dr/dt$. Rewriting and integrating equation (5) yields:

$$t_{n+1} - t_n = \frac{\beta ln(Q-r_n{}^2)}{2\alpha} - \frac{\beta ln(Q-r_{n+1}{}^2)}{2\alpha} \quad (7)$$

Solving for r_{n+1} gives:

$$r_{n+1} = \sqrt{\frac{Q-(Q-\pi(e+i)r_n^2)\exp(\frac{2\pi(e+i)}{2\pi h_c}(t_n-t_{n+1}))}{\pi(e+i)}} \quad (8)$$

By choosing a time step ($t_n - t_{n+1}$) and assigning a radial distance (r_1) for the first cell, equation (8) can then be used to calculate the lengths of the consecutive cells.

Total water loss was calculated by dividing the measured discharge by the size of the modern wetland environment. Rates for *e* and *i* were then calculated using the averaged proportions of previously published estimates for warmer and cooler periods (Chapter 4; Keppel et al., 2012b) and then multiplying by total water-loss. For the study presented in this chapter, 33% of water-loss was attributed to evapotranspiration and 67% to infiltration, which represents the average between results from warmer and cooler months (Chapter 4). Values for the discharge rate *Q* were assumed to be the equivalent of current-day *Q* values and were obtained either from saline dilution tests completed in October 2008 (Halihan pers. comm., 2008) or from temporary weir measurements (BHPB, 2005).

Finally, a sensitivity analysis of model parameters was undertaken to account for the uncertainty associated with the model parameters.

5.4 Results

5.4.1 Water chemistry results

A table of water quality measurements and chemistry analyses collected from each of the spring localities is provided as Table 5.2. The temperature of springwaters varied between 19.4°C and 30.4°C and electrical conductivity (EC) ranged between 2.5 and 7.9 mS/cm. The oxidation/reduction potential (ORP) indicated that with the exception of Blanche Cup (67.7 mV) and The Bubbler (4.9 mV), springwaters were generally reducing in character upon emergence (-10.0 to -138.9 mV). All alkalinities were greater than 400 mg/L ($CaCO_3$) and pH of springwater was generally near-neutral on emergence (6.9-7.4), with the exception being Beresford Spring (7.9). PCO_2 values for all emergent springwater were several orders of magnitude greater than average atmospheric values and SI_c ranged between -0.46 to 0.05, the exception was Beresford Spring (0.76). The relatively high alkalinity and SI_c results from Beresford spring suggest that CO_2 degassing from groundwater is more advanced at the point of emergence than other sites.

5.4.2 Modelling results

The model demonstrates that the maximum radius of a mound could be approximated using the calculated SI_c. The predicted radius was equal to the distance where the calculated SI_c falls below 0.05, which approximates the point where change in carbonate hydrochemistry are predicted to slow rapidly as $CaCO_3$ in solution nears equilibrium (Figure 5.4). In all cases, it was noted that this point was obtained before the maximum radius of the wetland (*R*) as defined using equation (5), although in the case of Billa Kalina the two were nearly coincident. Consequently, the initial mound footprint of these structures can be described as

primarily controlled by carbonate precipitation. This observation is best illustrated by a comparison between the fluid concentration of Ca^{2+} in springwater and fluid flow velocity as a percentage of the initial condition with respect to time (Figure 5.5). These data indicate that by the time approximately 95% of the discharging Ca^{2+} is predicted to have been precipitated (marking the point where carbonate precipitation decreases rapidly and consequently the edge of mound construction) water is anticipated to have only travelled approximately half (40 to 65%) of the calculated distance on the surface. The one exception was Billa Kalina where the rates of velocity decay and carbonate precipitation were comparable; this suggests that any change in environmental condition which may slow carbonate precipitation in these particular circumstances may lead mound construction to be "discharge" controlled, meaning that *R* may be obtained before $CaCO_3$ in solution can approach equilibrium conditions.

The size of the predicted mound footprints generally compared well to the mapped outline of the mounds (Table 5.3 and Figures 5.6 and 5.7). Such a finding is notable given the age of mound spring structures, which can range in excess of 700,000 years (Prescott and Habermehl, 2008) and that erosion and dissolution may affect the size of mound structures.

5.6 Discussion

The similarity of predicted and measured mound footprints based on broad assumptions concerning the long term springwater budget suggests that if reasonable assumptions concerning the hydrochemistry of groundwater can be made, the model may have use in estimating the discharge required to form relict mound spring structures.

The average radius of each mapped mound structure, calculated as if the surface area was circular, versus the model radius is shown in Figure 5.8. Large differences in the predicted and measured radius of mound structures could tentatively be used as an indication of changes in discharge rate since the time of initial formation. It is notable that the linear regression of data ($y = 0.82x$) displays a bias toward model under-prediction and that this was governed by the discrepancies found at Beresford Spring and Blanche Cup between predicted and measured mound radii (Figure 5.8 and Table 5.3) This is consistent with previously published theories presented by Linares et al., (2010), Pentecost (2005) and Williams and Holmes (1978) that suggest the rate of spring discharge slows as the mound height approaches that of the hydrostatic head. Such changes in spring discharge from the time of initial formation may also be attributable to several factors including a change in groundwater pressure within the aquifer via the development of new springs or flowing bores nearby, a change in the discharge capacity of the spring conduit via clogging or deformation of the spring conduit via tectonic activity.

Table 5.2: Water quality and chemistry results for the spring sites included in this study. All samples were taken from the spring vent.

Name	Date	Alk.	Temp	Sp. EC	pH	ORP	F^-	Cl^-	Br^-	SO_4^{2-}	Ca^{2+}	K^+	Mg^{2+}	Na^+	Si^{4+}	Sr^{2+}	PCO_2	SI_c
		$CaCO_3$	°C	mS/cm		mV											matm	
Beresford	Oct 08	580	20.7	6. 56	7.87	-10.0	1.20	1558	1.73	262	74.2	46.1	37.3	1335	7.56	2.51	7.4	0.76
Warburton	Mar 09	546	27.3	6. 05	7.06	-108.7	1.50	1470	1.60	277	80.1	43.3	38.4	1356	8.11	2.65	51.3	0.05
The Bubbler	Jul 09	814	30.4	2. 46	7.15	4.9	2.90	1204	2.80	127	36.7	32.7	28.3	1160	6.09	1.36	66.1	0.05
Blanche Cup	Apr 11	681	23.5	6.87	7.21	67.7	1.7	1900	1.90	330	46.7	29.9	37.1	1310	4.71	2.17	42.66	-0.46
Billa Kalina	Mar 09	416	23.9	7. 88	6.88	-138.9	0.34	2134	2.26	379	152.6	55.7	30.4	1745	5.49	4.18	53.7	-0.05

[a]All analytical determinations in mg/L unless otherwise stated.

Table 5.3: Comparison of estimated radii of mound structures from aerial photographic mapping and predicted radii from modelling.

Spring	Average water depth calculated (m)	Estimated average radius mound base (m)	Predicted radius from model (m)
Beresford	0.017	27.1	9.5
Warburton	0.047	46.2	43.1
The Bubbler	0.063	39.7	41.5
Blanche Cup	0.024	31.0	13.5
Billa Kalina	0.023	12.2	16.7

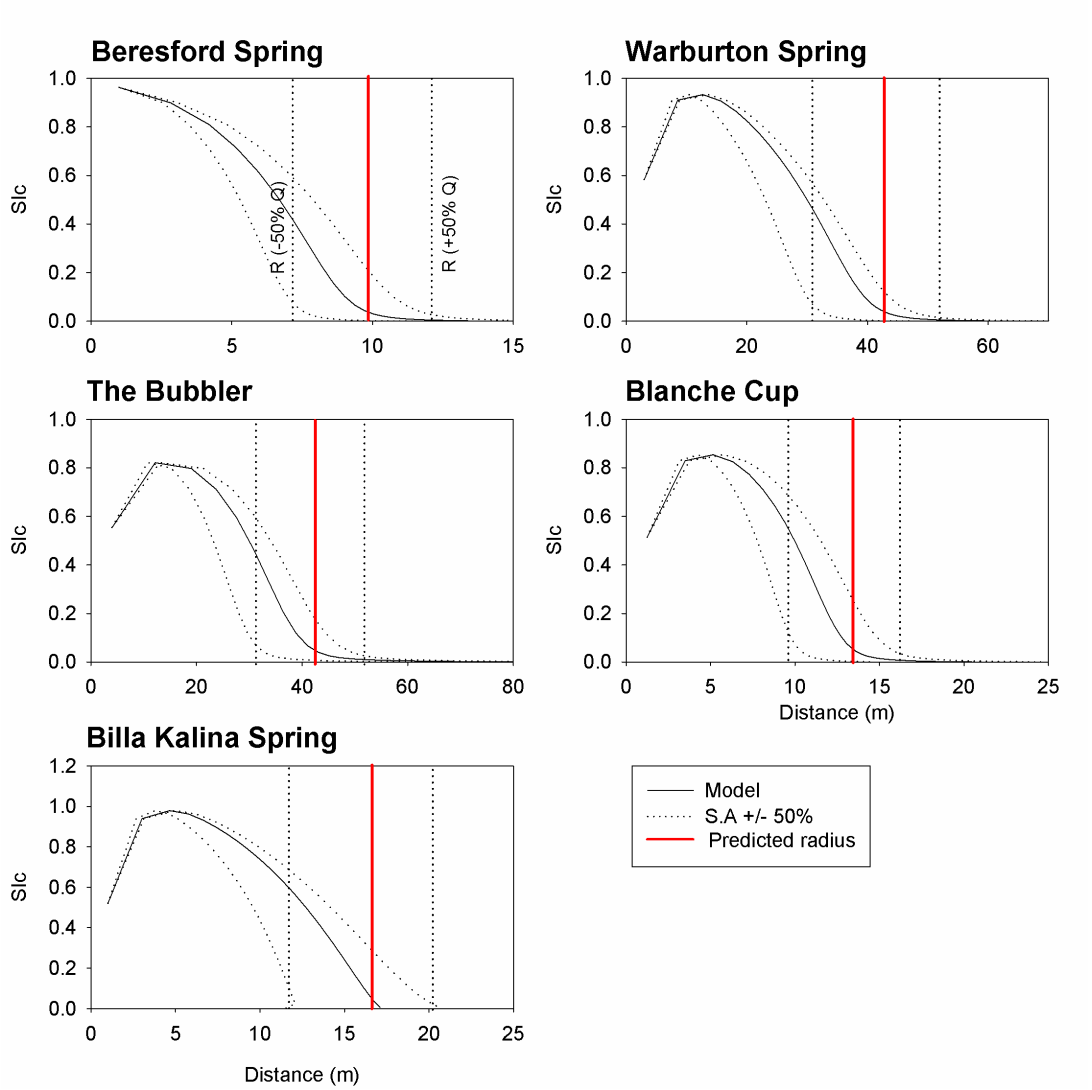

Figure 5.4: Graphs of SI_c calculations for spring examples. The predicted mound footprint radii are drawn as red line at the point where $SI_c < 0.05$. Dotted lines represent +/- 50% variations to discharge conducted as part of sensitivity analysis.

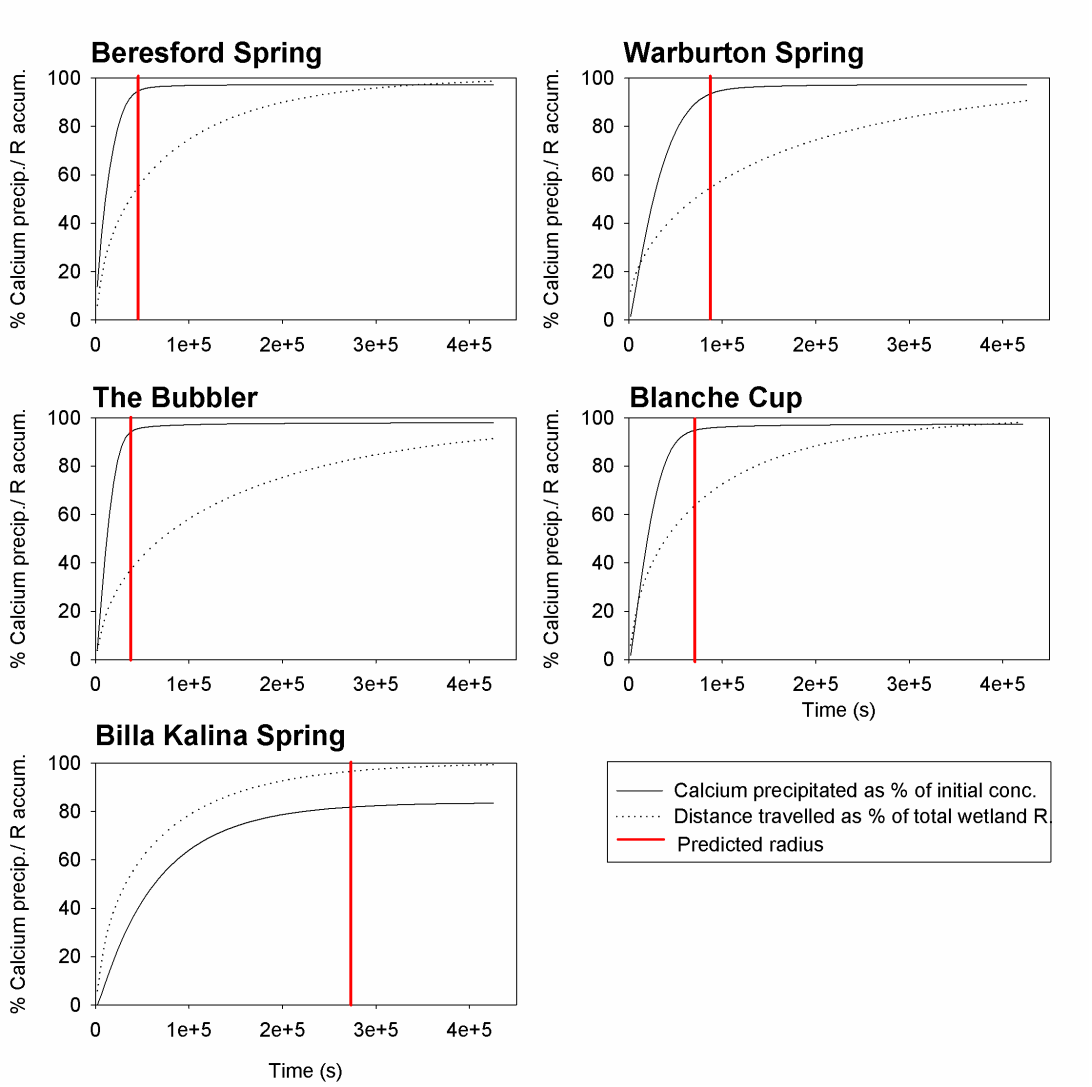

Figure 5.5: Graphs of Ca^{2+} precipitated as a percentage of the initial concentration and distance travelled by springwater as a percentage of the total wetland radius *R* with respect to time. The predicted mound footprint radius is drawn as red line at the point where $SI_c < 0.05$. Note that in all cases except Billa Kalina, the predicted radius of the mound footprint is reached well before water has reached the edge of the wetland. For Billa Kalina, the predicted mound footprint radius and the edge of the wetland are nearly coincident.

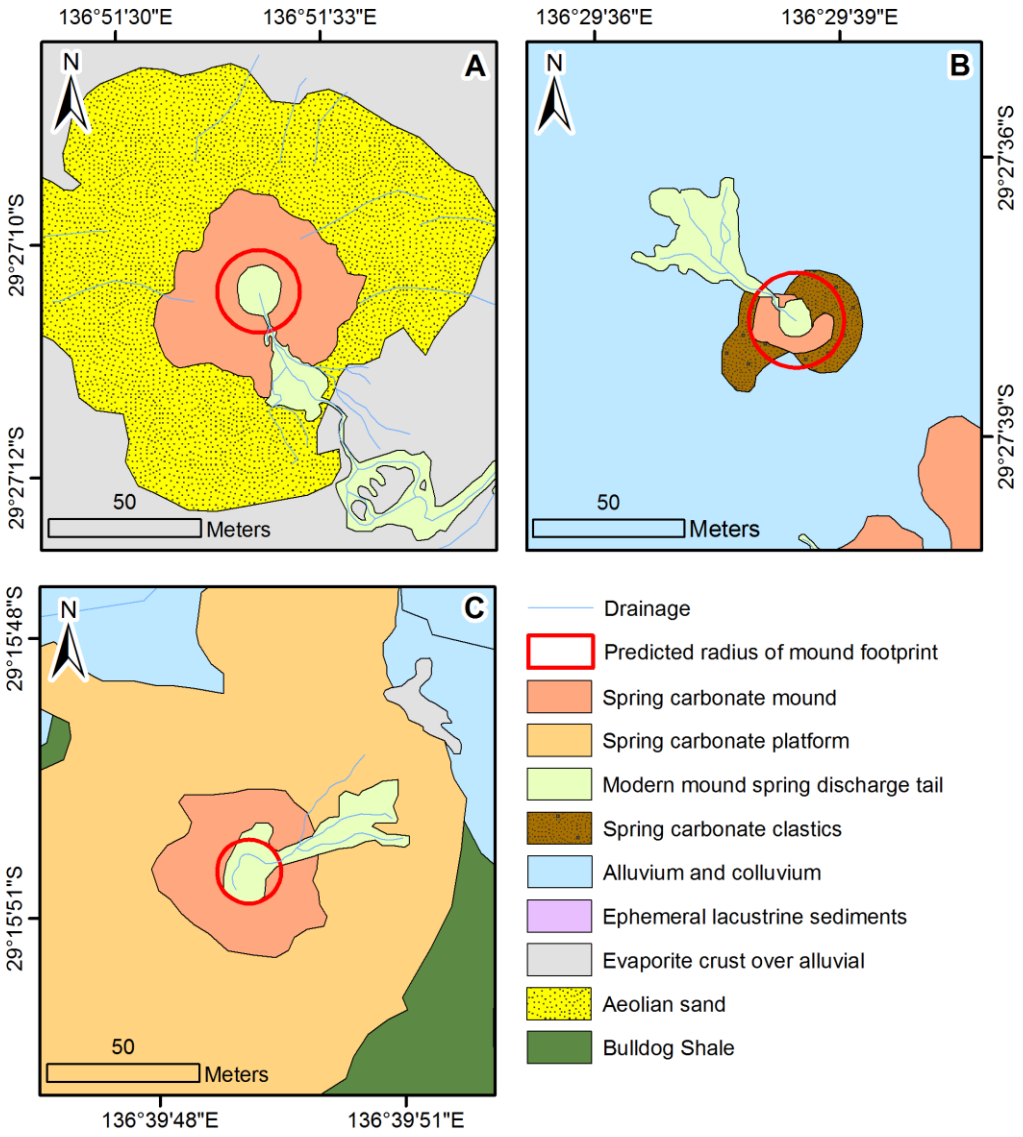

Figure 5.6: The predicted radius of water depletion for three mound spring environments with low discharge (<1 L/sec) compared to the geological and morphological interpretation. Study sites represented are A) Blanche Cup, Wabma Kadarbu NP Spring complex, B) Billa Kalina Spring and C) Beresford Spring, Beresford Hill Spring complex.

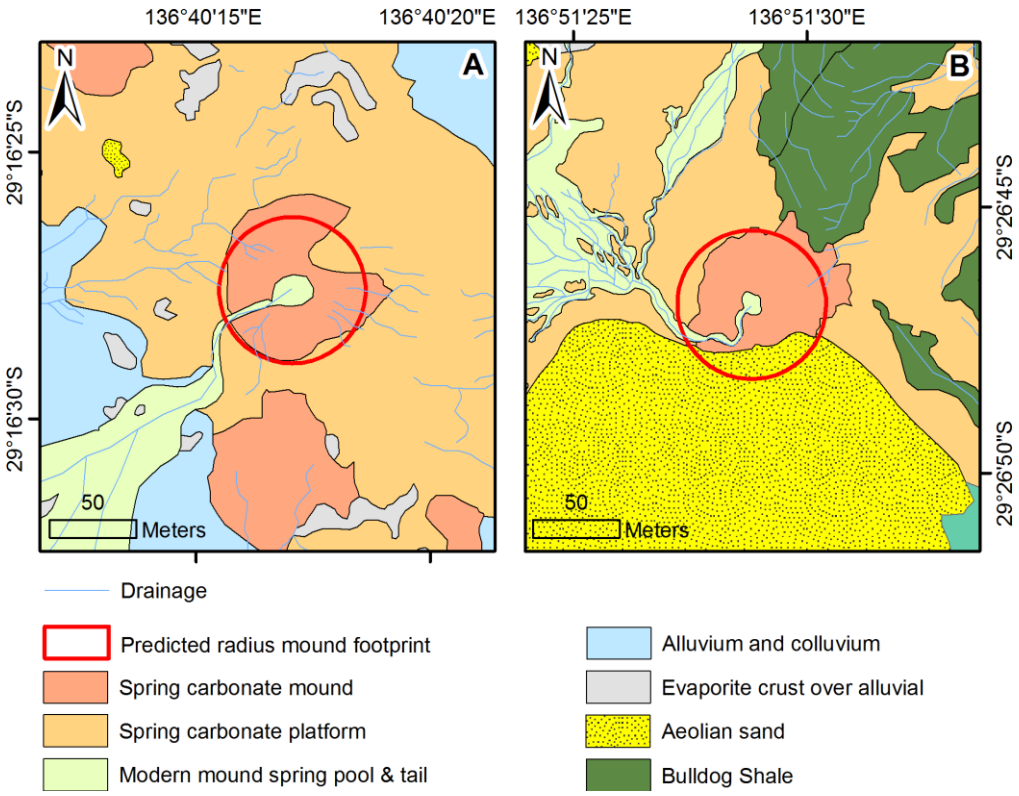

Figure 5.7: The predicted radius of carbonate precipitation for two mound spring environments with high discharge (>1 L/sec) compared to the geological and morphological interpretation. Study sites represented are: A) Warburton Spring, Beresford Hill Spring complex and B) The Bubbler, Wabma Kadarbu NP Spring complex.

Using the developed model, the predicted *Q* necessary to obtain the mound footprints at Blanche Cup and Beresford Spring estimated from mapping are 2.0 l/sec and 0.76 l/sec respectively. Such differences in discharge represent approximately an order of magnitude change in flow from the time of initial mound formation to the present day, although given the absolute values of *Q* involved, neither change seems implausible.

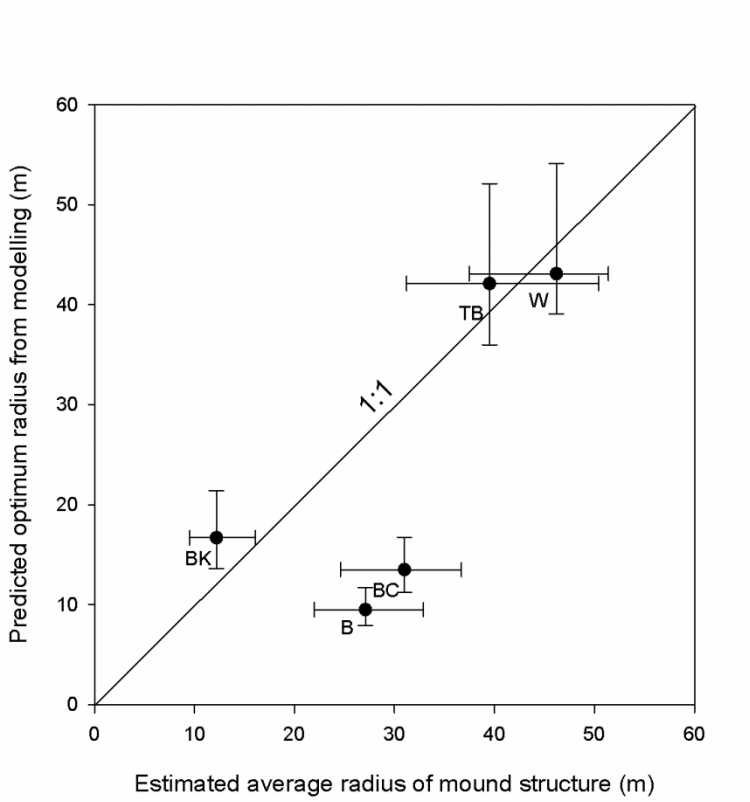

Figure 5.8: Scatter plot of the estimated average mapped radius of each mound structure versus the maximum radius carbonate precipitation as predicted by modelling. Vertical error bars represent predicted radii after +/-50% variations in *Q*. Horizontal error bars represent the difference between the minimum and maximum radii measured from the mound structures compared to the estimated average calculated radius (Table 5.3). A linear regression of $y = 0.81x$ (not shown) had an R^2 value of 0.56.

In cases where the predicted footprint from modelling was slightly larger than the measured mound footprint, partial destruction of the mound via erosion or dissolution may explain differences, particularly if the mound is radially asymmetrical (Figure 5.7B). Alternatively, widening of the spring conduit via dissolution or structural deformation may also result in increased discharge.

Obviously, the application of the model to past environments necessitates critical assumptions regarding past discharge and environmental conditions. This is particularly important where modelled estimates diverge notably from mapped

extents. Sensitivity analysis suggests the model to be most consistently sensitive to changes in the parameter Q and the related the value of h_c and consistently least sensitive to changes in e. A 50% variation in Q altered predicted mound radii between 9% and 28% (Figures 5.4).

Kadlec (1990) noted that wetland flow is strongly dependent on water depth; using equation (6) as a means of estimation, it was found that a 50% change in h_c would necessitate a change in Q of between 89% and 416%, resulting in changes to the predicted mound footprint radii of between 42 and 97%.

In contrast, a 50% change in e was found to alter the predicted mound radii between 0.2 and 7.2%, with the impact being greatest at Billa Kalina where the rates of carbonate precipitation and velocity decay are proportionally similar (Figure 5.5). Likewise, a 50% change in evapotranspiration and infiltration together ($e+i$) impacted the modelled prediction between 2 and 7% at all springs except Billa Kalina, where the impact was as high as 26%. It was also found that the impact of such changes to $e+i$ on h_c was negligible.

Variations in the parameters rc_T, alkalinity and Kw on the predicted mound radii had a notable proportionality with the influence of carbonate precipitation on mound footprint construction. At spring locations excluding Billa Kalina, a 50% change in rc_T and alkalinity impacted the predicted mound radii between 3 and 19% and 9 and 34% respectively. As a K_w value for dense vegetation was originally used, the sensitivity analysis was limited to using a calculated value for sparse vegetation coverage (5.0×10^7 /m.day), estimated from previously published field-based experiments from other wetland environments (Kadlec, 1990; Tsihrintzis and

Madiedo, 2000); use of this value resulted in an increase in the predicted radii of mounds excluding Billa Kalina of between 14 and 20%. At Billa Kalina, the maximum impact of 50% changes to rc_T, alkalinity and K_w were 2, 4 and 2% respectively.

Consequently, this sensitivity analysis suggests that potential impacts of climate change on mound construction are dependent on the supply of groundwater rather than variations in evapotranspiration or ambient conditions.

5.7 Conclusions

In summary, carbonate reactive transport modelling was able to potentially provide a quantitative framework in which the radius of a spring-related structure was estimated and was thus able to constrain past spring activities. Furthermore, deviations between predicted and measured mound radii have reasonable explanations related to the impact of environmental conditions on discharge and morphology. Consequently, this approach has potential application as a tool in both palaeohydrology and palaeoclimatology studies. Gross differences between predicted and actual morphology may be used to imply changes in discharge rate over time and potential changes in either the potentiometric surface or rate of groundwater recharge. Additionally, the footprint of calcareous mound spring structures is conceptualised as being primarily a product of carbonate precipitation, although the sensitivity of the model to discharge suggests this is also influential.

It is recognised that such hydrological systems are complex and that a number of factors may be responsible for such change; the expansion of this study with the inclusion of additional study sites is required to further substantiate the proof of concept presented here. Nevertheless, it is felt that the modelling approach provides a quantitative framework for the analysis of near-ambient temperature spring-related carbonate formations.